### Journal
ACS central science, 5(3)

### ISSN
2374-7943



### Authors
Oh, Hee Jeung
Aboian, Mariam S
Yi, Michael YJ
et al.



### Publication Date
2019-03-01

### DOI
10.1021/acscentsci.8b00700

Peer reviewed

ACS central science

Research Article

Cite This: ACS Cent. Sci. 2019, 5, 419−427

http://pubs.acs.org/journal/acscii

# 3D Printed Absorber for Capturing Chemotherapy Drugs before They Spread through the Body

Hee Jeung Oh,[†] Mariam S. Aboian,[#] Michael Y. J. Yi,[†] Jacqueline A. Maslyn,[†,∥] Whitney S. Loo,[†] Xi Jiang,[∥] Dilworth Y. Parkinson,[⊥] Mark W. Wilson,[#] Terilyn Moore,[#] Colin R. Yee,[#] Gregory R. Robbins,[∇] Florian M. Barth,[∇] Joseph M. DeSimone,[*,∇,○,◆] Steven W. Hetts,[*,#] and Nitash P. Balsara[*,†,‡,§,∥]

[†]Department of Chemical and Biomolecular Engineering, University of California, Berkeley, California 94720, United States

[‡]Energy Storage and Distributed Resources Division, [§]Joint Center for Energy Storage Research (JCESR), [∥]Materials Sciences Division, [⊥]Advanced Light Source Division, Lawrence Berkeley National Laboratory, Berkeley, California 94720, United States

[#]Department of Radiology, School of Medicine, University of California, San Francisco, California 94110, United States

[∇]Carbon, Inc., 1089 Mills Way, Redwood City, California 94063, United States

[○]Department of Chemistry, University of North Carolina, Chapel Hill, North Carolina 27599, United States

[◆]Department of Chemical and Biomolecular Engineering, North Carolina State University, Raleigh, North Carolina 27695, United States

*Supporting Information*

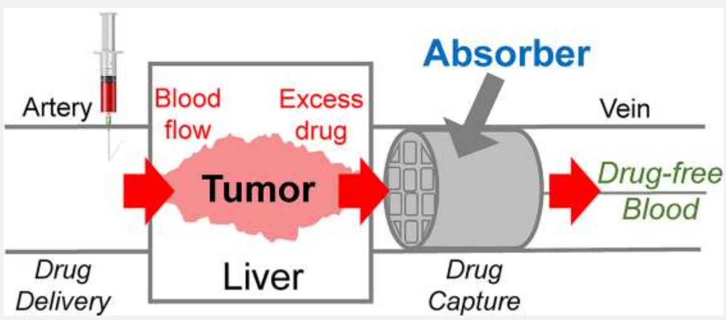


**ABSTRACT:** Despite efforts to develop increasingly targeted and personalized cancer therapeutics, dosing of drugs in cancer chemotherapy is limited by systemic toxic side effects. We have designed, built, and deployed porous absorbers for capturing chemotherapy drugs from the bloodstream after these drugs have had their effect on a tumor, but before they are released into the body where they can cause hazardous side effects. The support structure of the absorbers was built using 3D printing technology. This structure was coated with a nanostructured block copolymer with outer blocks that anchor the polymer chains to the 3D printed support structure and a middle block that has an affinity for the drug. The middle block is polystyrenesulfonate which binds to doxorubicin, a widely used and effective chemotherapy drug with significant toxic side effects. The absorbers are designed for deployment during chemotherapy using minimally invasive image-guided endovascular surgical procedures. We show that the introduction of the absorbers into the blood of swine models enables the capture of 64 ± 6% of the administered drug (doxorubicin) without any immediate adverse effects. Problems related to blood clots, vein wall dissection, and other biocompatibility issues were not observed. This development represents a significant step forward in minimizing toxic side effects of chemotherapy.

## INTRODUCTION

Cancer is becoming the leading cause of death in most developed nations.[1,2] Although there have been enormous efforts to develop more targeted and personalized cancer therapeutics, dosing of drugs in cancer chemotherapy is often limited by systemic toxic side effects. During intra-arterial chemotherapy infusion to a target organ,[3,4] excess drug that is not trapped in the target organ passes through to the veins draining the organ, and is then circulated to the rest of the body, causing toxicities in distant locations. Typically, more than 50−80% of the injected drug is *not* trapped in the target organ, bypasses the tumor, and enters general circulation.[5]

In the context of reducing the toxicity of chemotherapy, we present the development of a new biomedical device: an absorber that captures excess chemotherapeutic drug before it spreads through the body.[6−9] Absorption columns are routinely used in industry to remove pollutants from chemical streams.

**Received:** October 1, 2018
**Published:** January 9, 2019

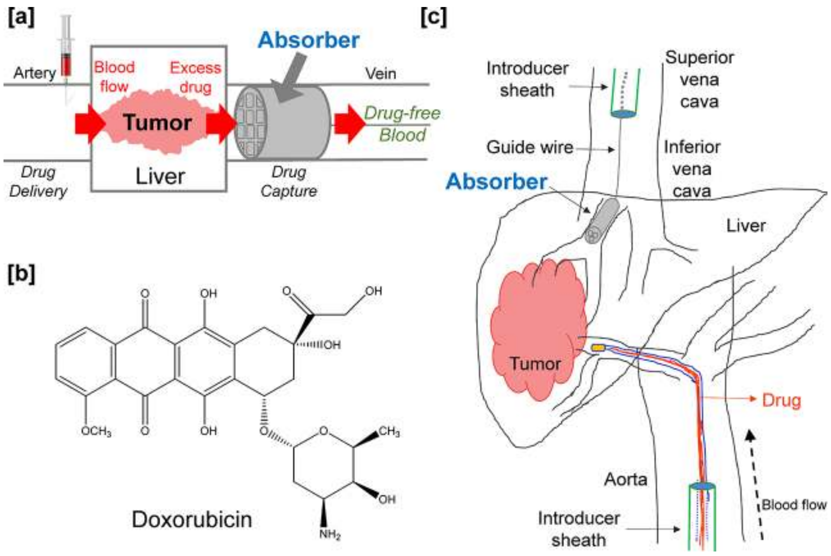


**Figure 1.** (a) Diagram showing the proposed approach for drug capture using a 3D printed absorber. (b) Chemical structure of doxorubicin, the chemotherapy drug used in this study. (c) Schematic of the endovascular treatment of liver cancer by administering intra-arterial chemotherapy via the hepatic artery. The excess drug is captured by the proposed absorber in the vein draining the organ. The introducer sheath used to guide the absorber to the desired location via a minimally invasive endovascular approach is also shown.

The proposed absorber is temporarily deployed in the vein draining the organ undergoing intra-arterial chemotherapy infusion, and is removed after the infusion is completed. This concept is depicted schematically in Figure 1a where we show the treatment of a tumor within the liver. The drug is injected in the hepatic artery as is the case in conventional intra-arterial chemotherapy infusion. The blood exiting the liver through the hepatic veins passes through the absorber that, in principle, captures the excess drug. In principle, if all of the drug is not captured during the first pass, some of it may be captured at subsequent passes. The particular drug used in this study is doxorubicin. The chemical structure of doxorubicin is shown in Figure 1b. The proposed approach for doxorubicin capture is shown in Figure 1c. Minimally invasive image-guided endovascular surgical procedures are used to deliver the drug to the tumor using the hepatic artery and to place the absorber in the hepatic veins, hepatic vein confluence, or suprahepatic inferior vena cava. The standard introducer sheaths and guide wires used to accomplish this task are shown in Figure 1c. The approach described in Figure 1 can be used to minimize toxic effects of chemotherapy used at different locations in the body. The toxicity of drugs used to treat other diseases besides cancer may also be modulated by the proposed approach. Similarly, toxins from bacterial infections, environmental toxins, or cells themselves could be captured using specific chemical, physical, or biological features.[10−12]

Doxorubicin is a low-cost, highly effective agent frequently used in chemotherapy for several decades.[13] Based on a linear dose response model, increasing the dose of doxorubicin linearly increases tumor cell death.[14−24] This provides motivation for higher-dose doxorubicin therapy, but the side effects of high-dose doxorubicin therapy include irreversible cardiac failure, which limits implementation of the high-dose regimen. An established and highly effective agent like doxorubicin is a compelling first candidate for demonstrating the proposed drug capture approach.

For the absorber to work efficiently, it must selectively bind the target drug (doxorubicin in this study) within an hour or less (typical time scale of intra-arterial chemotherapy infusion for the liver). The structure of the absorber must be carefully designed and fabricated so as not to severely impair blood flow or cause thrombosis, although the latter issue is easily addressed with intraprocedural anticoagulation, a standard technique in interventional radiology. Custom-made absorbers must be used as individual patients have veins of different dimensions. We have thus used 3D printing to fabricate the absorbers used in this study. Successful design, fabrication, and deployment of the absorber has the potential to open a new route to help patients fight cancer.

## RESULTS AND DISCUSSION

Porous cylinders, shown in Figure 2, were printed at Carbon, Inc. in Redwood City, CA.[25] The absorbers were 5 mm in diameter and 30 mm in length. The targeted internal structure of the cylinders is shown in Figure 2a. A central hole (diameter = 0.89 mm) that runs through the cylinder enables attachment of a device to a guide wire needed for minimally invasive surgery. This is surrounded by a square lattice structure with a characteristic dimension of 800 $\mu$m. This dimension was chosen to prevent hemolysis of blood cells; white blood cells, with diameters about 9−20 $\mu$m, are the largest component of blood.[26,27] The porous cylinders were printed by photoinduced cross-linking of poly(ethylene glycol) diacrylate (PEGDA), shown in Figure 2c. Poly(ethylene glycol)-based polymers are widely used in biomedical engineering because of their biocompatibility and fouling resistance.[28−34] Moreover, other relevant properties such as mechanical strength and water swelling of PEG-based polymers can be readily tuned by controlling the polymerization conditions.[35−44] Optical micrographs of the 3D printed porous cylinders are shown in Figure 2b. It is clear that the printing process faithfully reproduces the targeted internal structures shown in Figure 2a. The porous cylinder serves as the scaffold of the absorber.

The surfaces of the porous cylinders were coated with a poly(*tert*-butylstyrene)-*b*-poly(ethylene-*co*-propylene)-*b*-poly(styrene-*co*-styrenesulfonate)-*b*-poly(ethylene-*co*-propylene)-*b*-poly(*tert*-butylstyrene) (PtBS−PEP−PSS−PEP−PtBS) block copolymer provided by Kraton Performance Polymers, Inc.


DOI: 10.1021/acscentsci.8b00700
ACS Cent. Sci. 2019, 5, 419−427

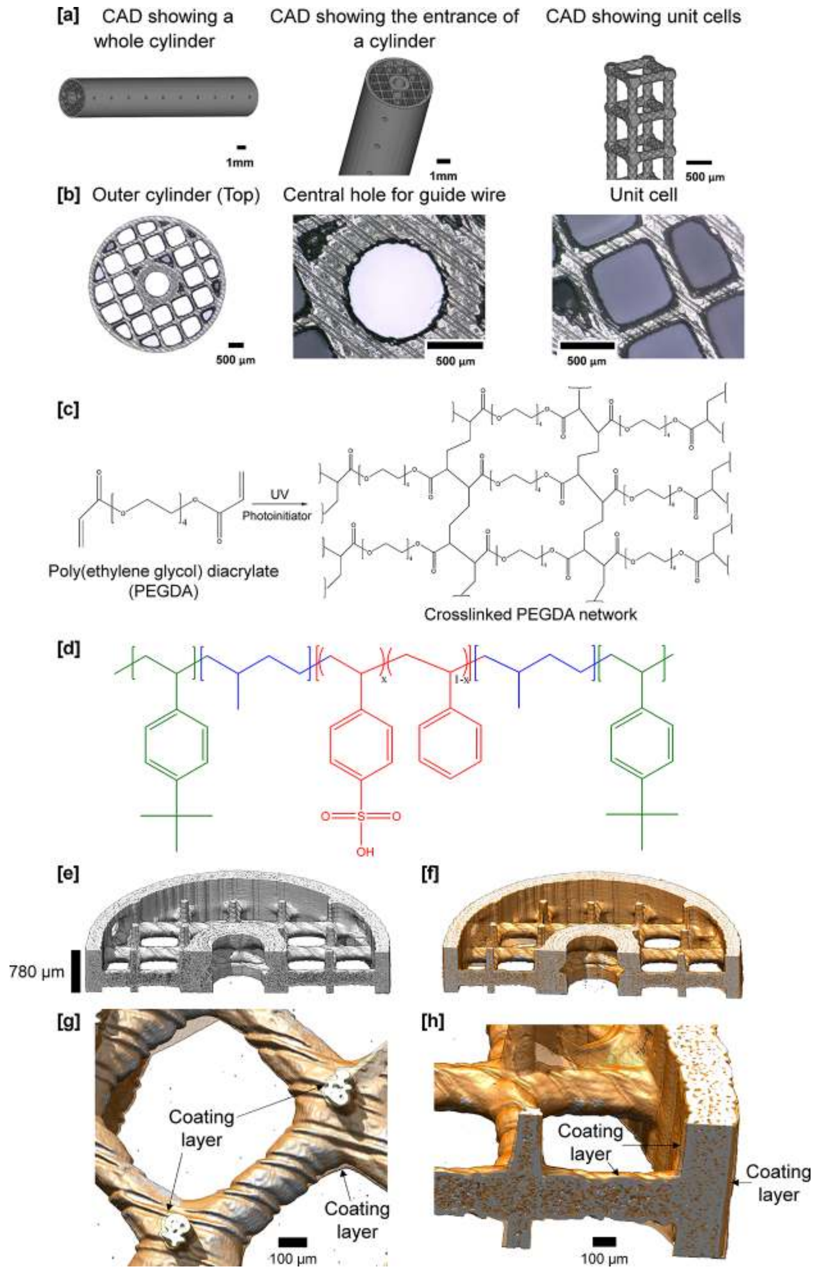


**Figure 2.** (a) Drawing of the 3D printed porous cylinder using computer-aided design (CAD). (b) Optical micrographs of a typical 3D printed porous cylinder. (c) Chemical reaction used in the 3D printer: cross-linking of poly(ethylene glycol) diacrylate. The cylinder serves as a scaffold for the surface coating necessary for drug capture. (d) Chemical structure of the PtBS−PEP−PSS−PEP−PtBS block copolymer used in this study. (e) 3D reconstruction from X-ray microtomography of the uncoated scaffold. (f) Superposed 3D reconstruction of uncoated (gray) and coated (orange) absorbers and (g, h) magnified views at different locations. The arrows denote the block copolymer coating layer.

(Houston, TX). The chemical structure of the block copolymer is shown in Figure 2d. The block copolymer was provided in the form of 10 wt % solution of the polymer dissolved in a mixture of heptane and cyclohexane (72:28 by mass).[45−47] The 3D printed cylinders were fitted into silicone tubing, and the polymer solution was pumped through the cylinders for 10 min. The cylinders were then dried, first in air at 50 °C for 1 h and 30 min, followed by drying under vacuum at room temperature for 24 h. This resulted in a coating of the copolymer on the printed cylinders. To visualize this coating, the surface-modified cylinders were imaged using phase-contrast X-ray microtomography. The X-ray microtomography experiment was designed to image three sets of lattices at a time. An uncoated filter was imaged first, and the image obtained is shown in Figure 2e. The internal structure within the scaffolds seen in Figure 2e may arise due to either voids or noisy data. The same filter was subjected to the coating protocol and imaged again by phase-contrast X-ray microtomography. The two tomograms were superposed, and voxels in the tomogram of the coated absorber were colored in orange, while the uncoated filter voxels were colored in gray. The superposed tomogram, shown in Figure 2f, clearly shows the presence of a uniform coating over the surfaces of the absorber. The magnified image of the lattice struts, shown in Figure 2g, h, shows the thickness of the coated layer at several locations. The X-ray microtomography experiments confirm the presence of a reasonably homogeneous coating of the PtBS−


DOI: 10.1021/acscentsci.8b00700
ACS Cent. Sci. 2019, 5, 419−427

PEP−PSS−PEP−PtBS polymer on the absorber scaffolds. The coating thickness is more-or-less uniform, ranging from 30 to 60 $\mu$m. The estimated surface area of an absorber is 2000 $mm^2$ including an external surface. Additional X-ray tomography slices and confocal microscopy images of uncoated and coated absorbers are shown in the Supporting Information (Figures S1 and S2). Our choice for the polymer coating was informed by previous studies where it was shown that polystyrenesulfonate chains demonstrated high capacity for binding with doxorubicin.[6,8,9] It is likely that the PtBS and PEP blocks in the block copolymer are responsible for adhesion between the coating and 3D printed scaffold. The approach for coating the cylinders described here was arrived at after considerable trial and error. Small changes in the composition of either the block copolymer or the solvent result in unstable coating on the scaffolds.

We performed *in vivo* experiments with the coated 3D printed absorbers described above in three animal models (swine). The diameter of the absorbers (5 mm) was determined by the size of the introducer sheath (i.e., 18 French or 6 mm diameter sheath) that could be accommodated in the common femoral and common iliac veins of the swine, which are similar in diameter to the hepatic veins in an adult human. The diameter of the introducer sheath is minimized to minimize blood loss during the operation. The length of the absorbers (30 mm) was chosen to match the length of the common iliac vein. The common iliac vein was chosen to facilitate interpretation of experimental data and demonstrate proof-of-concept. Also, the diameter of the common iliac vein is approximately 10 mm, similar to the diameter of human hepatic veins near their confluence with the inferior vena cava where the absorbers will be placed for capturing excess drug draining the liver during hepatic intra-arterial chemotherapy infusion (see Figure 1c). To minimize the blood flow around the absorber, two cylinders were brought to the desired location using the introducer sheath, one after the other, and arranged in parallel as shown in Figure 3a.

The absorbers were tested in the swine models undergoing chemo-infusion in the common iliac vein of 50 mg of doxorubicin over 10 min, corresponding to a typical dose used clinically in chemotherapy for intra-arterial treatment of hepatocellular carcinoma. Doxorubicin concentrations were monitored as a function of time using blood-sampling catheters at three different locations. Two locations, the pre-device and post-device sampling catheters, are depicted schematically in Figure 3a. The pre-device catheter is located between the injection and the absorber. The post-device catheter is located just after the absorber. The third catheter was located at the internal jugular vein, well-removed from the common iliac vein such that any blood sample taken from this location will reflect the systemic drug concentration, as doxorubicin would have had to pass through the inferior vena cava, heart, pulmonary vasculature, systemic arteries, capillaries, and systemic veins to reach that sampling point. We refer this as the peripheral location. X-ray fluoroscopy images of the absorbers in common iliac vein obtained during one of our *in vivo* experiments are shown in Figure 3b, c. The introduction sheath and guide wires used to deliver the absorbers are clearly seen in Figure 3b. The sheath was introduced via a common femoral vein. The absorbers are located between metallic fasteners that are also visible in Figure 3b. The higher-magnification image (Figure 3c) shows the two absorbers arranged in parallel.

Results of two separate *in vivo* experiments are shown in Figure 4. In Figure 4a, we show the measured doxorubicin concentration as a function of time at the three locations

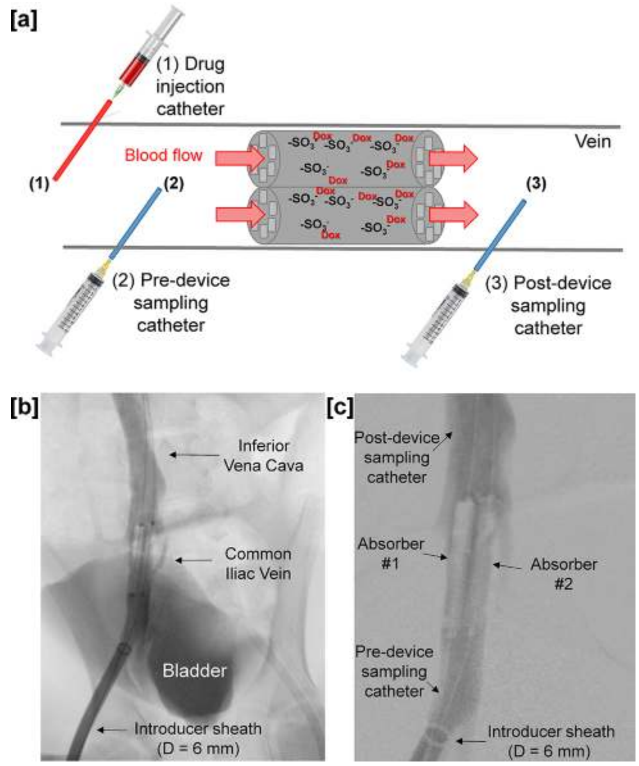


**Figure 3.** (a) Schematic of the *in vivo* experiments showing two absorbers placed in a vein, and catheters used for drug injection and for measurement of doxorubicin (Dox) concentration at the pre-device and post-device sampling locations. (b, c) Fluoroscopy images taken during the *in vivo* experiments showing two absorbers aligned in parallel in the common iliac vein. (c) Magnified view showing two absorbers.

described above during a control experiment, wherein uncoated absorbers were placed in the common iliac vein. The doxorubicin concentrations measured at the pre-device and the post-device locations are qualitatively similar, indicating that most of the doxorubicin injected passes through the absorbers. In both cases, the doxorubicin concentration increases rapidly at early time, remains well above the background for about 10−15 min, and then decreases to zero at about 30 min. The doxorubicin concentration measured at the peripheral location increases only slightly when doxorubicin is injected into the animal model. In Figure 4b, we show the images of the plasma from the centrifuged samples obtained from the three sampling catheters during the control experiments. Since doxorubicin has a characteristic orange color, the higher the doxorubicin concentration is, the darker the orange color is in the samples. The color darkness in the samples is qualitatively consistent with the doxorubicin concentration profiles shown in Figure 4a. There is little qualitative difference between the images obtained from the pre-device and the post-device catheters in the control experiment.

In Figure 4c, we show the measured doxorubicin concentration as a function of time when coated absorbers were deployed. These results differ significantly from those in Figure 4a. In Figure 4c, we see that the post-device doxorubicin concentration is significantly lower than that measured at the pre-device location. The integrated areas under the two data sets enable quantification of the drug capture efficiency. In this experiment, 69% of the doxorubicin is captured by the coated 3D printed absorbers, corresponding to 0.017 mg doxorubicin/$mm^2$ of surface. The images of the plasma from the centrifuged



DOI: 10.1021/acscentsci.8b00700
ACS Cent. Sci. 2019, 5, 419−427

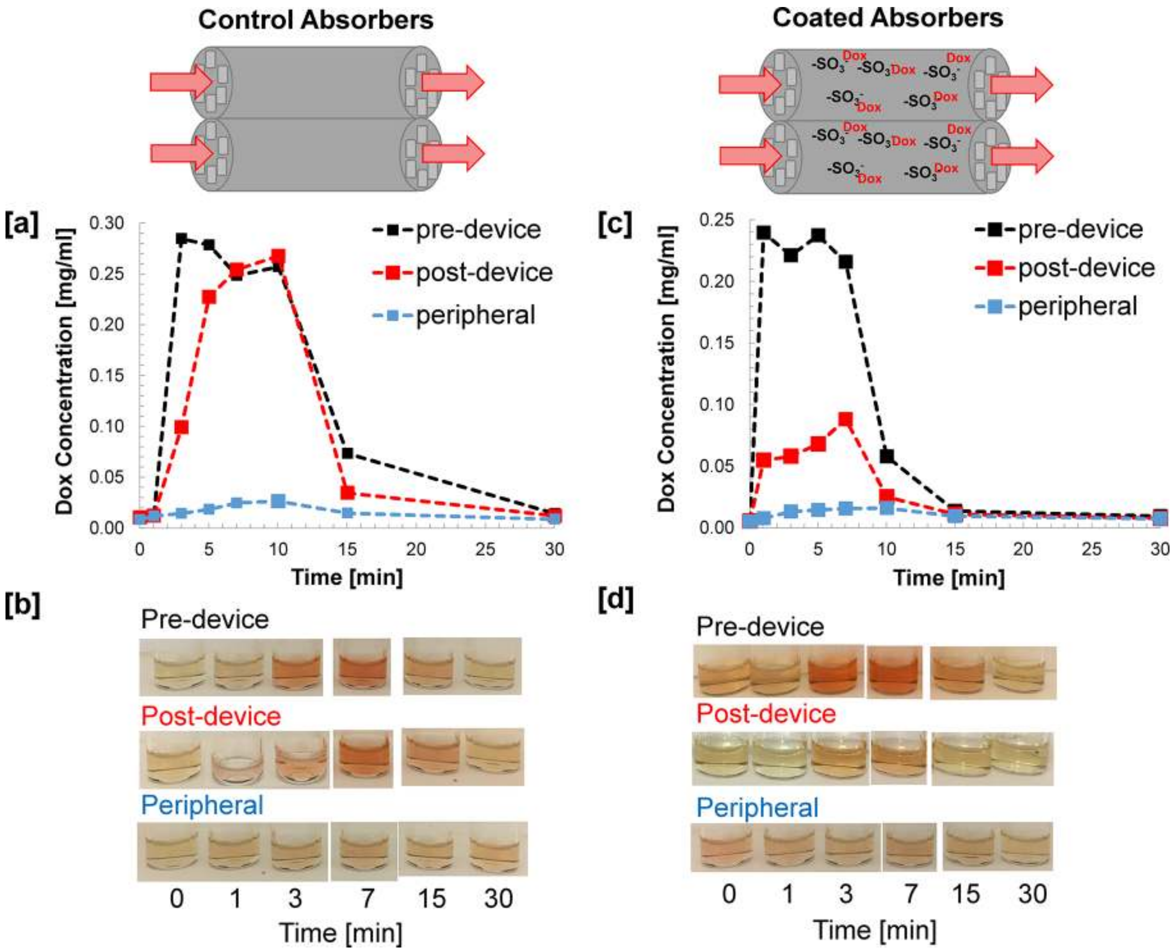


**Figure 4.** Results of *in vivo* drug capture experiments. Schematic of the placement of absorbers in the common iliac vein: (left) two control absorbers without coating and (right) two coated absorbers. Doxorubicin concentration as a function of time at three different sampling locations of (a) two control absorbers without coating and (c) two coated absorbers. Photographs of plasma from the centrifuged samples obtained from (b) two control absorbers without coating and (d) two coated absorbers.

samples obtained from three sampling catheters during this experiment, shown in Figure 4d, confirm the removal of doxorubicin. In addition, problems related to blood clots, vein wall dissection, and other biocompatibility issues were not observed during the operation.

The experiments described above (using two coated and two uncoated absorbers in parallel as shown in Figure 4) were repeated in two additional animals. In one of the animals, the experiments with the coated absorbers were performed two times. The trends of the other drug capture experiments were similar to those reported in Figure 4 (absolute Dox concentrations differ by a factor of about two). The results of other drug capture experiments are shown in the Supporting Information (Figures S3 and S4). The doxorubicin capture efficiency ranged from 57% to 69%. The average value of drug capture efficiency was 64 ± 6%.

After the *in vivo* experiments, we tried to release the doxorubicin from the coated absorbers by pumping an aqueous potassium chloride and ethanol mixture (20% w/v)[48−52] through the absorbers for one month. Analysis of the mixture showed negligible doxorubicin concentrations (less than 0.001 mg/mL). This implies that doxorubicin binds irreversibly to the absorbers. Following this experiment, the absorbers were crushed and immersed in the aqueous mixture of potassium chloride and ethanol described above. The uncoated absorbers used in *in vivo* experiments were subjected to the same experiments. The results of this experiment are shown in Figure 5. A colorless solution was obtained when the uncoated absorbers, used in *in vivo* experiments, were studied, as shown in Figure 5a. In contrast, an orange colored solution was obtained when the coated absorbers, used in *in vivo* experiments,

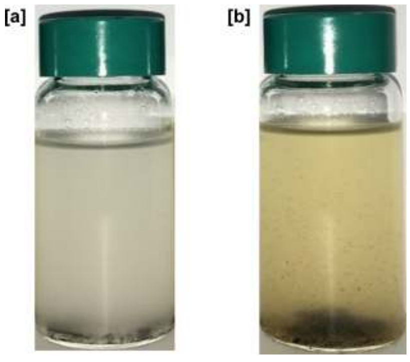


**Figure 5.** Photographs of aqueous mixtures of potassium chloride and ethanol after addition of crushed absorbers used in *in vivo* experiments: (a) control experiment with uncoated absorbers and (b) experiments with two coated absorbers. The orange color in part b is due to the presence of captured doxorubicin.



DOI: 10.1021/acscentsci.8b00700
ACS Cent. Sci. 2019, 5, 419−427

were studied, as shown in Figure 5b. If doxorubicin were only present in the coating, it would have been relatively easy to extract it after the *in vivo* experiments. We thus posit that doxorubicin is trapped in the interior of our absorbers. From a practical point of view, this may be advantageous, as it implies, that doxorubicin will not be released into the body as the absorbers are withdrawn through the blood vessels after the proposed chemotherapy procedure is completed. From an analytical point of view, however, it has proven difficult to quantify the amount of doxorubicin that has been absorbed. Significant further work is required to quantify this.

## ■ CONCLUSION

We have designed, built, and deployed porous absorbers for capturing chemotherapy drugs *in vivo* before they spread through the body to reduce systemic toxic side effects. The porosity of the absorber was obtained by 3D printing a lattice structure within the cylinders. The application of a polystyrenesulfonate coating on the absorber was essential for drug capture. Our initial design enables the capture of 64 ± 6% of the administered drug without noticeable adverse side effects. There are numerous approaches for using the platform we have developed to improve the efficacy of drug capture. Most simply, the number of absorber devices could be increased, increasing total surface area for drug binding. The lattice size could also be decreased to enhance drug capture. Additional improvement in performance may be obtained by changing the chemical composition and thickness of the coating layer. Absorbers developed here could be used in conjunction with other approaches for delivering chemotherapy drug such as drug-eluting-bead-based transarterial chemoembolization (TACE).[49,51,53−56] In future clinical trials, we may use custom 3D printed elastomeric absorbers with patient-specific form factors that fit optimally in the vein(s) of the patient, as can be created from preprocedure computed tomography (CT) or magnetic resonance imaging (MRI) data sets. Although much work remains, we believe that the present study opens a new route to help patients fight cancer by minimizing drug toxicity, and better treat their disease and improve survival by enabling high-dose regional chemotherapy.

## ■ MATERIALS AND METHOD

**Preparation of Porous Cylinders.** Cylindrical porous absorbers for this study were prepared at Carbon, Inc., a 3D printing company located at Redwood City, CA. The prepolymer solution was prepared by adding 1 wt % initiators (i.e., 0.8 wt % of 2,4,6-trimethylbenzoyl-diphenylphosphine oxide (TPO, Sigma-Aldrich) and 0.2 wt % of 2-isopropylthioxanthone (ITX, Esstech, Inc.)) and 0.23 wt % of carbon black pigment to poly(ethylene glycol) diacrylate (PEGDA, MW = 250 g/mol, Sigma-Aldrich) (see Figure 2c). The solution was photopolymerized by using the continuous liquid interface production (CLIP) method; more information about the CLIP can be found elsewhere.[25,57−59] The cylinders obtained by this process were washed in 2-propanol to remove uncured resin from the polymer network. The cylinders were allowed to air-dry after washing and were UV postcured using a Dymax ECE 5000 UV cure chamber (Torrington, CT) in 30 s intervals with rotation in-between cures for a total of 2 min. Absorbers were imaged and measured using a Keyence VHX-5000 microscope (Itasca, IL).

**Sulfonated Polymer Used for Coating on Porous Cylinders.** The surface of the 3D printed porous cylinders was modified by coating a thin layer of sulfonated styrenic pentablock copolymers. The sulfonated styrenic pentablock copolymers (PtBS−PEP−PSS−PEP−PtBS) were synthesized via anionic polymerization and a subsequent postpolymerization sulfonation process, and detailed procedures have been described elsewhere.[60,61] The sulfonation level (mol %) of the middle polystyrene (PS) block was controlled to a desired ion exchange capacity (IEC). In this study, the sulfonated pentablock copolymer of IEC = 2.0 mequiv/g (dry polymer) (sulfonation level = 52 mol %) was used. The number-average molecular weight of the unsulfonated pentablock copolymer is approximately 78 000 g/mol (block mass fractions are PtBS:PEP:PSS = 0.33:0.27:0.40), and the volume fraction of mid PSS block is 0.434[45,46]. Water uptake in this copolymer, measured by soaking films in water at room temperature until equilibrium was reached (up to a week), was 1.44 ± 0.01 g of water per g of dry polymer.

**X-ray Tomography.** The uncoated and coated absorbers were imaged using synchrotron hard X-ray microtomography at beamline 8.3.2 of the Advanced Light Source at Lawrence Berkeley National Laboratory. X-rays with energy 23 keV were generated by the synchrotron and illuminated the sample. The X-rays transmitted through the sample were converted using a scintillator into visible light. The X-ray beam was over 10 mm in width. The position of the sample with respect to the X-ray beam was chosen so that three sets of struts in the absorber could be imaged in one scan. The sample to detector distance was 150 mm, and the X-ray exposure time was 300 ms. This image was magnified by an optical microscope and collected on a sCMOS pco.edge detector. As the sample was rotated through 180°, a total of 2160 images were collected.[31] These projection images were reconstructed using the tomography plugin for the program Xi-Cam,[62] which uses TomoPy[63] to generate digital cross-sectional slice images, and subsequently these were stacked to generate 3D reconstructed images of the cylinders. The superpositions of 3D reconstructed uncoated and coated cylinders were performed using the fit-in-map method of the UCSF Chimera package (correlation factor = 0.99).[64]

***In Vivo* Experiments.** 3D printed absorbers were tested *in vivo* in three swine models (40−45 kg). The absorber was strung along a polytetrafluoroethylene (PTFE) coated nitinol guide wire (Glidewire, Terumo Interventional Systems, Somerset, NJ) for smooth and rapid movement through tortuous blood vessels; The guide wire went through the middle hole of the absorber, and two metallic fasteners on each end of the absorber were used to keep the absorber in place. *In vivo* experiments were performed under compliance with the protocols of the Institutional Animal Care and Use Committee (IACUC) at the University of California, San Francisco (UCSF). Each animal was monitored with blood pressure, pulse oximetry, heart rate, and electrocardiogram while under general anesthesia with isoflurane. An 18 French (diameter = 6 mm) introducer sheath (Gore Dryseal Flex Introducer Sheath, W. L. Gore & Associates, Inc., Flagstaff, AR) placed into the common femoral vein was used to deliver the absorbers into the common iliac vein. Sampling and injection catheters were placed under fluoroscopy guidance at the spot of interest relative to the absorbers. A pre-device sampling catheter was introduced via the sheath to the left common iliac vein. A post-device sampling catheter was introduced through the internal jugular vein and was placed into the common iliac vein adjacent to the bifurcation of the


DOI: 10.1021/acscentsci.8b00700
ACS Cent. Sci. 2019, 5, 419−427

vena cava. The distances between the catheters and absorbers were carefully adjusted to be consistent over a series of *in vivo* experiments. Prior to the start of the experiments, patency of the venous system was demonstrated using iodinated contrast injection (Iohexol, Omnipaque-300, GE Healthcare).

To simulate intra-arterial chemotherapy dosing, 50 mg of doxorubicin (2 mg/mL, doxorubicin hydrochloride injection, United States Pharmacopeia, Pfizer, New York, NY) was injected into the common iliac vein via an infusion pump at a constant rate of 2.5 mL/min over 10 min. Blood aliquots of 2 mL at different times from the pre-device, post-device, and peripheral sampling locations were collected after 1.5 mL of blood was wasted to account for the volume within the catheter.

**Measurement of Doxorubicin Concentration.** Doxorubicin concentrations in the blood aliquots were determined using fluorescence spectroscopy. The blood aliquots were first centrifuged to separate the plasma from other blood components, since the majority of doxorubicin is in the plasma.[9] Fluorescence measurements were made using the plasma samples to determine the doxorubicin concentration. The fluorescence measurements were made using a FlexStation 3 Multi-Mode microplate reader (Molecular Devices, San Jose, CA) at a known emission wavelength of 550 nm upon excitation with a 480 nm laser.[6,8,9,48−51,65] The excitation and emission wavelengths are based on well-established protocols in determining doxorubicin concentration.[8,9] The doxorubicin concentration was calculated from the measured fluorescence at 550 nm using the calibration curve, which correlates fluorescence emission to doxorubicin concentration.

## ■ ASSOCIATED CONTENT

### Supporting Information

The Supporting Information is available free of charge on the ACS Publications website at DOI: 10.1021/acscentsci.8b00700.

Additional information on X-ray microtomography of absorbers and results of *in vivo* drug capture experiments (PDF)

## ■ AUTHOR INFORMATION


### Corresponding Authors

*Phone: (650) 285-6307; (919) 962-2166. E-mail: joe@carbon3d.com; desimone@unc.edu.
*Phone: (415) 206-6607. E-mail: Steven.Hetts@ucsf.edu.
*Phone: (510) 642-8973. E-mail: nbalsara@berkeley.edu.

### ORCID

Hee Jeung Oh: 0000-0003-1846-9547
Jacqueline A. Maslyn: 0000-0002-6481-2070
Whitney S. Loo: 0000-0002-9773-3571
Xi Jiang: 0000-0002-9589-7513
Dilworth Y. Parkinson: 0000-0002-1817-0716
Nitash P. Balsara: 0000-0002-0106-5565


### Notes

The authors declare the following competing financial interest(s): J.M.D. is the co-founder/CEO of and has an equity stake in Carbon, Inc., a 3D printing company commercializing continuous liquid interface production (CLIP) technology. G.R.R. is an employee, and F.M.B. is a former employee of Carbon, Inc. Carbon, Inc. is the manufacturer of CLIP equipment. CLIP is protected under issued US patents including 9,205,601, 9,211,678, and 9,216,546. S.W.H. and M.W.W. are the co-inventors of an in vivo positionable filtration device and methods related thereto to enable chemotherapy delivery in a targeted manner (WO/2014/100201).

Safety statement: no unexpected or unusually high safety hazards were encountered. Problems related to blood clots, vein wall dissection, and other biocompatibility issues were not observed during the operation.

## ■ ACKNOWLEDGMENTS

This work was supported by National Institute of Health (NIH) and National Cancer Institute (NCI) under Project 5R01CA194533-03. M.S.A. is supported by National Institutes of Health Biomedical Imaging and Bioengineering T32 under Grant 5T32EB001631-12. Sample preparation and data processing for X-ray microtomography was supported by the Soft Matter Electron Microscopy Program (KC11BN), supported by the Office of Science, Office of Basic Energy Science, US Department of Energy, under Contract DE-AC02-05CH11231. Work at the Molecular Foundry and the Advanced Light Source at Lawrence Berkeley National Laboratory was supported by the Office of Science, Office of Basic Energy Sciences, of the U.S. Department of Energy under Contract DE-AC02-05CH11231. The graphics and analyses of X-ray tomography were performed with the UCSF Chimera package. Chimera is developed by the Resource for Biocomputing, Visualization, and Informatics at the University of California, San Francisco (supported by NIGMS P41-GM103311). We would like to thank Dr. Carl Willis and Dr. Richard Blackwell at the Kraton Performance Polymers, Inc. for kindly donating materials for this study. We are grateful to Dr. Ronald Zuckermann and Dr. Behzad Rad of the Molecular Foundry at Lawrence Berkeley National Laboratory for their help and support with characterization. We also would like to thank Ms. Carol Stillson of the University of California, San Francisco for her support during *in vivo* experiments.

## ■ REFERENCES

(1) Siegel, R. L.; Miller, K. D.; Jemal, A. Cancer statistics, 2017. *Ca-Cancer J. Clin.* **2017**, *67* (1), 7−30.

(2) Kochanek, K. D.; Murphy, S. L.; Xu, J.; Arias, E. *Mortality in the United States, 2016*; National Center for Health Statistics (NCHS) Data Briefs, 2017; Vol. *293*, December, pp 1−7.

(3) Roche, A.; Girish, B. V.; de Baere, T.; Baudin, E.; Boige, V.; Elias, D.; Lasser, P.; Schlumberger, M.; Ducreux, M. Trans-catheter arterial chemoembolization as first-line treatment for hepatic metastases from endocrine tumors. *Eur. Radiol* **2003**, *13* (1), 136−140.

(4) Stuart, K. Chemoembolization in the management of liver tumors. *Oncologist* **2003**, *8* (5), 425−37.

(5) Hwu, W. J.; Salem, R. R.; Rosenblatt, M.; D'Andrea, E.; Leffert, J. J.; Faraone, S.; Marsh, J. C.; Pizzorno, G. A clinical-pharmacological evaluation of percutaneous isolated hepatic infusion of doxorubicin in patients with unresectable liver tumors. *Oncology Research* **1999**, *11* (11−12), 529−537.

(6) Chen, X. C.; Yang, J.; Chin, A.; Patel, A. S.; Hetts, S. W.; Balsara, N. P. *Copolymer membrane for high-dose chemotherapy delivery during transarterial chemoemblization*. U.S. Patent 20160101218A1, 2015.

(7) Hetts, S. W.; Patel, A. S.; Wilson, M. W. *In vivo positionable filtration devices and method related thereto*, Patent WO 2014/100201 A1, 2014.

(8) Chen, X. C.; Oh, H. J.; Yu, J. F.; Yang, J. K.; Petzetakis, N.; Patel, A. S.; Hetts, S. W.; Balsara, N. P. Block copolymer membranes for efficient capture of a chemotherapy drug. *ACS Macro Lett.* **2016**, *5* (8), 936−941.

(9) Patel, A. S.; Saeed, M.; Yee, E. J.; Yang, J.; Losey, A. D.; Lillaney, P. V.; Thorne, B.; Chin, A. K.; Malik, S.; Wilson, M. W.; Chen, X. C.; Balsara, N. P.; Hetts, S. W. Development and validation of endovascular



DOI: 10.1021/acscentsci.8b00700
*ACS Cent. Sci.* 2019, 5, 419−427

chemotherapy filter device for removing high-dose doxorubicin: preclinical study. *Journal of Medical Devices* **2014**, *8* (4), 041008–410088.
(10) Mabray, M. C.; Lillaney, P.; Sze, C. H.; Losey, A. D.; Yang, J.; Kondapavulur, S.; Liu, D.; Saeed, M.; Patel, A.; Cooke, D.; Jun, Y. W.; El-Sayed, I.; Wilson, M.; Hetts, S. W. In Vitro Capture of Small Ferrous Particles with a Magnetic Filtration Device Designed for Intravascular Use with Intraarterial Chemotherapy: Proof-of-Concept Study. *Journal of Vascular and Interventional Radiology* **2016**, *27* (3), 426–432.
(11) Kondapavulur, S.; Cote, A. M.; Neumann, K. D.; Jordan, C. D.; McCoy, D.; Mabray, M. C.; Liu, D.; Sze, C. H.; Gautam, A.; VanBrocklin, H. F.; Wilson, M.; Hetts, S. W. Optimization of an endovascular magnetic filter for maximized capture of magnetic nanoparticles. *Biomed. Microdevices* **2016**, *18* (6), 109.
(12) Aboian, M. S.; Yu, J. F.; Gautam, A.; Sze, C. H.; Yang, J. K.; Chan, J.; Lillaney, P. V.; Jordan, C. D.; Oh, H. J.; Wilson, D. M.; Patel, A. S.; Wilson, M. W.; Hetts, S. W. In vitro clearance of doxorubicin with a DNA-based filtration device designed for intravascular use with intra-arterial chemotherapy. *Biomed. Microdevices* **2016**, *18* (6), 98.
(13) Doroshaw, J. Anthracyclines and Anthracenediones. In *Cancer Chemotherapy and Biotherapy: Principles and Practice (Chabner, Cancer Chemotherapy and Biotherapy)*; Chabner, B. A., Longo, D. L., Eds.; Lippincott Williams & Wilkins: Philadelphia, 1996; pp 409–434.
(14) August, D. A.; Verma, N.; Vaerten, M. A.; Shah, R.; Andrews, J. C.; Brenner, D. E. Pharmacokinetic evaluation of percutaneous hepatic venous isolation for administration of regional chemotherapy. *Surg Oncol* **1995**, *4* (4), 205–16.
(15) Curley, S. A.; Newman, R. A.; Dougherty, T. B.; Fuhrman, G. M.; Stone, D. L.; Mikolajek, J. A.; Guercio, S.; Guercio, A.; Carrasco, C. H.; Kuo, M. T.; et al. Complete hepatic venous isolation and extracorporeal chemofiltration as treatment for human hepatocellular carcinoma: a phase I study. *Ann. Surg Oncol* **1994**, *1* (5), 389–99.
(16) Hwu, W. J.; Salem, R. R.; Pollak, J.; Rosenblatt, M.; D'Andrea, E.; Leffert, J. J.; Faraone, S.; Marsh, J. C.; Pizzorno, G. A clinical-pharmacological evaluation of percutaneous isolated hepatic infusion of doxorubicin in patients with unresectable liver tumors. *Oncol Res.* **1999**, *11* (11–12), 529–537.
(17) Ku, Y.; Tominaga, M.; Iwasaki, T.; Fukumoto, T.; Muramatsu, S.; Kusunoki, N.; Sugimoto, T.; Suzuki, Y.; Kuroda, Y.; Saitoh, Y. Efficacy of repeated percutaneous isolated liver chemoperfusion in local control of unresectable hepatocellular carcinoma. *Hepatogastroenterology* **1998**, *45* (24), 1961–1965.
(18) Ku, Y.; Iwasaki, T.; Fukumoto, T.; Tominaga, M.; Muramatsu, S.; Kusunoki, N.; Sugimoto, T.; Suzuki, Y.; Kuroda, Y.; Saitoh, Y.; Sako, M.; Matsumoto, S.; Hirota, S.; Obara, H. Induction of long-term remission in advanced hepatocellular carcinoma with percutaneous isolated liver chemoperfusion. *Ann. Surg.* **1998**, *227* (4), 519–26.
(19) Ku, Y.; Iwasaki, T.; Fukumoto, T.; Tominaga, M.; Muramatsu, S.; Kusunoki, N.; Sugimoto, T.; Suzuki, Y.; Kuroda, Y.; Saitoh, Y. Percutaneous isolated liver chemoperfusion for treatment of unresectable malignant liver tumors: technique, pharmacokinetics, clinical results. *Recent Results Cancer Res.* **1998**, *147*, 67–82.
(20) Ravikumar, T. S.; Pizzorno, G.; Bodden, W.; Marsh, J.; Strair, R.; Pollack, J.; Hendler, R.; Hanna, J.; D'Andrea, E. Percutaneous hepatic vein isolation and high-dose hepatic arterial infusion chemotherapy for unresectable liver tumors. *J. Clin. Oncol.* **1994**, *12* (12), 2723–36.
(21) Ku, Y.; Tominaga, M.; Iwasaki, T.; Fukumoto, T.; Kuroda, Y. Isolated hepatic perfusion chemotherapy for unresectable malignant hepatic tumors. *Int. J. Clin Oncol* **2002**, *7* (2), 82–90.
(22) Walker, M. C.; Parris, C. N.; Masters, J. R. Differential sensitivities of human testicular and bladder tumor cell lines to chemotherapeutic drugs. *Journal of the National Cancer Institute* **1987**, *79* (2), 213–216.
(23) Skipper, H. E.; Schabel, F. M. J.; Mellett, L. B.; Montgomery, J. A.; Wilkoff, L. J.; Lloyd, H. H.; Brockman, R. W. Implications of biochemical, cytokinetic, pharmacologic, and toxicologic relationships in the design of optimal therapeutic schedules. *Cancer Chemotherapy Reports* **1970**, *54* (6), 431–450.
(24) Porrata, L. F.; Adjei, A. A. The pharmacologic basis of high dose chemotherapy with haematopoietic stem cell support for solid tumours. *Br. J. Cancer* **2001**, *85* (4), 484–489.
(25) Tumbleston, J. R.; Shirvanyants, D.; Ermoshkin, N.; Janusziewicz, R.; Johnson, A. R.; Kelly, D.; Chen, K.; Pinschmidt, R.; Rolland, J. P.; Ermoshkin, A.; Samulski, E. T.; DeSimone, J. M. Continuous liquid interface production of 3D objects. *Science* **2015**, *347* (6228), 1349–1352.
(26) Prinyakupt, J.; Pluempitiwiriyawej, C. Segmentation of white blood cells and comparison of cell morphology by linear and naïve Bayes classifiers. *BioMedical Engineering OnLine* **2015**, *14* (63), 1–19.
(27) Sun, T. Introduction. In *Atlas of Hematologic Neoplasms*; Sun, T., Ed.; Springer: Boston, MA, 2009; pp 3–31.
(28) Bae, M. S.; Kwon, I. K. Photocurable hydrogel for tissue regeneration. In *Handbook of Intelligent Scaffolds for Tissue Engineering and Regenerative Medicine*; Khang, G., Ed.; Panstanford Publishing Pte. Ltd., 2012.
(29) Harris, J. M. *Poly(Ethylene Glycol) Chemistry: Biotechnical and Biomedical Applications*; Springer US, 1992.
(30) Andrade, J. D.; Hlady, V.; Jeon, S. I. Polyethylene oxide and protein resistance: principles, problems, and possibilities. In *Polymeric Materials Science and Engineering, Proceedings of the ACS Division of Polymeric Materials Science and Engineering*; I, A., Ed.; 1993; Vol. *69*, pp 60–61.
(31) Lee, J. H.; Lee, H. B.; Andrade, J. D. Blood compatibility of polyethylene oxide surfaces. *Prog. Polym. Sci.* **1995**, *20* (6), 1043–1079.
(32) Gölander, C. G.; Herron, J. N.; Lim, K.; Claesson, P.; Stenius, P.; Andrade, J.D. Properties of Immobilized PEG Films and the Interaction with Proteins. In *Poly(Ethylene Glycol) Chemistry*; Harris, J.M., Ed.; Springer: Boston, MA, 1992; pp 221–245.
(33) Nagaoka, S.; Nakao, A. Clinical application of antithrombogenic hydrogel with long poly (ethylene oxide) chains. *Biomaterials* **1990**, *11* (2), 119–121.
(34) Harris, J. M.; Dust, J. M.; Andrew McGill, R.; Harris, P. A.; Edgell, M. J.; Sedaghat-Herati, R. M.; Karr, L. J.; Donnelly, D. L. New Polyethylene Glycols for Biomedical Applications. In *Water-Soluble Polymers: Synthesis, Solution Properties, and Applications (ACS Symposium Series)*; Shalaby, S. W., McCormick, C. L., Butler, G. B., Eds.; ACS Publications, 1991; Vol. *467*, pp 418–429.
(35) Lin, H.; Kai, T.; Freeman, B. D.; Kalakkunnath, S.; Kalika, D. The Effect of Cross-Linking on Gas Permeability in Cross-Linked Poly(Ethylene Glycol Diacrylate). *Macromolecules* **2005**, *38* (20), 8381–8393.
(36) Lin, H.; Freeman, B. D. Gas Permeation and Diffusion in Cross-Linked Poly(ethylene glycol diacrylate). *Macromolecules* **2006**, *39* (10), 3568–3580.
(37) Emami, S. H.; Salovey, R. Crosslinked poly(ethylene oxide) hydrogels. *J. Appl. Polym. Sci.* **2003**, *88* (6), 1451–1455.
(38) Shekunov, B. Y.; Chattopadhyay, P.; Tong, H. H.; Chow, A. H.; Grossmann, J. G. Structure and drug release in a crosslinked poly(ethylene oxide) hydrogel. *J. Pharm. Sci.* **2007**, *96* (5), 1320–1330.
(39) Hennink, W. E.; van Nostrum, C. F. Novel crosslinking methods to design hydrogels. *Adv. Drug Delivery Rev.* **2012**, *64*, 223–236.
(40) Drury, J. L.; Mooney, D. J. Hydrogels for tissue engineering: scaffold design variables and applications. *Biomaterials* **2003**, *24* (24), 4337–4351.
(41) Peppas, N. A.; Keys, K. B.; Torres-Lugo, M.; Lowman, A. M. Poly(ethylene glycol)-containing hydrogels in drug delivery. *J. Controlled Release* **1999**, *62* (1–2), 81–87.
(42) Zhu, J. Bioactive modification of poly(ethylene glycol) hydrogels for tissue engineering. *Biomaterials* **2010**, *31* (17), 4639–4656.
(43) Mironi-Harpaz, I.; Wang, D. Y.; Venkatraman, S.; Seliktar, D. Photopolymerization of cell-encapsulating hydrogels: Crosslinking efficiency versus cytotoxicity. *Acta Biomater.* **2012**, *8* (5), 1838–1848.
(44) Revzin, A.; Russell, R. J.; Yadavalli, V. K.; Koh, W.-G.; Deister, C.; Hile, D. D.; Mellott, M. B.; Pichko, M. V. Fabrication of Poly(ethylene glycol) Hydrogel Microstructures Using Photolithography. *Langmuir* **2001**, *17* (18), 5440–5447.


DOI: 10.1021/acscentsci.8b00700
ACS Cent. Sci. 2019, 5, 419–427

(45) Choi, J.-H.; Willis, C. L.; Winey, K. I. Structure-property relationship in sulfonated pentablock copolymers. *J. Membr. Sci.* **2012**, *394–395*, 169–174.

(46) Geise, G. M.; Falcon, L. P.; Freeman, B. D.; Paul, D. R. Sodium chloride sorption in sulfonated polymers for membrane applications. *J. Membr. Sci.* **2012**, *423–424*, 195–208.

(47) Choi, J.-H.; Kota, A.; Winey, K. I. Micellar morphology in sulfonated pentablock copolymer solutions. *Ind. Eng. Chem. Res.* **2010**, *49* (23), 12093–12097.

(48) Swaine, T.; Tang, Y.; John, J.; Waters, L. J.; Lewis, A. L. Evaluation of ion exchange processes in drug-eluting embolization beads by use of an improved flow-through elution method. *Eur. J. Pharm. Sci.* **2016**, *93*, 351–359.

(49) Lewis, A. L.; Gonzalez, M. V.; Lloyd, A. W.; Hall, B.; Tang, Y.; Willis, S. L.; Leppard, S. W.; Wolfenden, L. C.; Palmer, R. R.; Stratford, P. W. DC bead: in vitro characterization of a drug-delivery device for transarterial chemoembolization. *Journal of Vascular and Interventional Radiology* **2006**, *17*, 335–342.

(50) Gonzalez, M. V.; Tang, C. Y.; Phillips, G. J.; Lloyd, A. W.; Hall, B.; Stratford, P. W.; Lewis, A. L. Doxorubicin eluting beads-2: methods for evaluating drug elution and in-vitro:in-vivo correlation. *J. Mater. Sci.: Mater. Med.* **2008**, *19* (2), 767–775.

(51) Hecq, J. D.; Lewis, A. L.; Vanbeckbergen, D.; Athanosopoulos, A.; Galanti, L.; Jamart, J.; Czuczman, P.; Chung, P. Doxorubicin-loaded drug-eluting beads (DC Bead®) for use in transarterial chemoembolization: a stability assessment. *J. Oncol. Pharm. Pract.* **2013**, *19* (1), 65–74.

(52) Namur, J.; Wassef, M.; Millot, J. M.; Lewis, A. L.; Manfait, M.; Laurent, A. Drug-eluting beads for liver embolization: concentration of doxorubicin in tissue and in beads in a pig model. *Journal of Vascular and Interventional Radiology* **2010**, *21* (2), 259–267.

(53) Vogl, T. J.; Gruber, T.; Balzer, J. O.; Euchler, K.; Hammerstingl, R.; Zangos, S. Repeated Transarterial Chemoembolization in the Treatment of Liver Metastases of Colorectal Cancer: Prospective Study. *Radiology* **2009**, *250* (1), 281–289.

(54) Sacco, R.; Bargellini, I.; Bertini, M.; Bozzi, E.; Romano, A.; Petruzzi, P.; Tumino, E.; Ginanni, B.; Federici, G.; Cioni, R.; Metrangolo, S.; Bertoni, M.; Bresci, G.; Parisi, G.; Altomare, E.; Capria, A.; Bartolozzi, C. Conventional versus doxorubicin-eluting bead transarterial chemoembolization for hepatocellular carcinoma. *J. Vasc Interv Radiol* **2011**, *22* (11), 1545–52.

(55) Buijs, M.; Vossen, J. A.; Frangakis, C.; Hong, K.; Georgiades, C. S.; Chen, Y.; Liapi, E.; Geschwind, J. F. Nonresectable hepatocellular carcinoma: long-term toxicity in patients treated with transarterial chemoembolization–single-center experience. *Radiology* **2008**, *249* (1), 346–54.

(56) Vogl, T. J.; Naguib, N. N.; Nour-Eldin, N. E.; Eichler, K.; Zangos, S.; Gruber-Rouh, T. Transarterial chemoembolization (TACE) with mitomycin C and gemcitabine for liver metastases in breast cancer. *Eur. Radiol* **2010**, *20* (1), 173–80.

(57) DeSimone, J. M.; Phelps, N. K. *Method and apparatus for three-dimensional fabrication with gas injection through carrier*. U.S. Patent 20170173880A1, 2014.

(58) DeSimone, J. M.; Ermoshkin, A.; Samulski, E. T. *Method and apparatus for three-dimensional fabrication*. U.S. Patent 9498920B2, 2013.

(59) DeSimone, J. M.; Ermoshkin, A.; Ermoshkin, N.; Samulski, E. T. *Continuous liquid interphase printing*. Patent WO2014126837A1, 2013.

(60) Willis, C. L.; Handlin, Jr., D. L.; Trenor, S. R.; Mather, B. D. *Process for preparing sulfonated block copolymers and various uses for such block copolymers*. U.S. Patent 8003733B2, 2011.

(61) Willis, C. L.; Handlin, Jr., D. L.; Trenor, S. R.; Mather, B. D. *Sulfonated block copolymers, method for making same, and various uses for such block copolymers*. Patent WO2007010039A1, 2010.

(62) Pandolfi, R. J.; Allan, D. B.; Arenholz, E.; Barroso-Luque, L.; Campbell, S. I.; Caswell, T. A.; Blair, A.; De Carlo, F.; Fackler, S.; Fournier, A. P.; Freychet, G.; Fukuto, M.; Gursoy, D.; Jiang, Z.; Krishnan, H.; Kumar, D.; Kline, R. J.; Li, R.; Liman, C.; Marchesini, S.; Ren, F.; Sahoo, S.; Strzalka, J.; Sunday, D.; Tassone, C. J.; Ushizima, D.; Venkatakrishnan, S.; Yager, K. G.; Zwart, P.; Sethian, J. A.; Hexemer, A. Xi-cam: A versatile interface for data visualization and analysis. *J. Synchrotron Radiat.* **2018**, *25* (4), 1261–1270.

(63) Gürsoy, D.; De Carlo, F.; Xiao, X.; Jacobsen, C. Tomopy: a framework for the analysis of synchrotron tomographic data. *J. Synchrotron Radiat.* **2014**, *21* (5), 1188–1193.

(64) Pettersen, E. F.; Goddard, T. D.; Huang, C. C.; Couch, G. S.; Greenblatt, D. M.; Meng, E. C.; Ferrin, T. E. UCSF Chimera–a visualization system for exploratory research and analysis. *J. Comput. Chem.* **2004**, *25* (13), 1605–1612.

(65) Motlagh, N. S. H.; Parviz, P.; Ghasemi, F.; Atyabi, F. Fluorescence properties of several chemotherapy drugs: doxorubicin, paclitaxel and bleomycin. *Biomed. Opt. Express* **2016**, *7* (6), 2400–2406.




DOI: 10.1021/acscentsci.8b00700
*ACS Cent. Sci.* 2019, 5, 419–427